

Figure 1. Hfq and bS21-2 influence production of T6SS proteins via different pathways. (A) Cells lacking bS21-2 have more Hfq. Bottom: Immunoblots probed with anti-VSV-G antibody. Whole cell lysates from bacteria containing Hfq-VSV-G and either with (WT) or without ($\Delta rpsU2$) bS21-2, in biological triplicate. Top: Quantification of immunoblots. Band intensities for each protein were normalized to total protein per lane on the membrane. **(B)** Loss of bS21-2 leads to more *hfq* translation. Relative fluorescence is reported for translational fusion reporters containing the 5' UTR of either *hfq* or *tul4* fused to *gfp* in cells with (WT) or without ($\Delta rpsU2$) bS21-2, in biological triplicate. Values relative to WT for each 5' UTR are shown. **(C)** Only some of the T6SS proteins are influenced by loss of Hfq. Bottom: Immunoblots probed with antibodies to indicated T6SS proteins in lysates of WT cells, cells lacking bS21-2 ($\Delta rpsU2$), or cells lacking Hfq (Δhfq). Top: Quantification of immunoblots. Band intensities for each protein were normalized to total protein per lane on the membrane. **(D)** Hfq does not influence translation of the T6SS protein PdpA. Relative fluorescence is reported for translational fusion reporters containing the 5' UTR of either *pdpA* or *tul4* fused to *gfp* in WT cells, cells lacking bS21-2 ($\Delta rpsU2$), or cells lacking Hfq (Δhfq), in biological triplicate. **(E)** Hfq is a negative regulator of T6SS gene transcript abundance. Quantitative real-time PCR was used to determine the relative transcript abundance for indicated FPI-encoded genes in WT cells, cells lacking bS21-2 ($\Delta rpsU2$), or cells lacking Hfq (Δhfq), normalized to the *tul4* gene. The *rpoA1* and *bfr* genes are included as additional negative controls, as their expression is not meaningfully influenced by bS21-2. (A-E) Error bars represent 1 SD. Experiments were repeated at least twice and data from a representative experiment are shown. (A-D) * $p < 0.05$ after Bonferroni correction. (E) * $p < 0.005$ after Bonferroni correction.

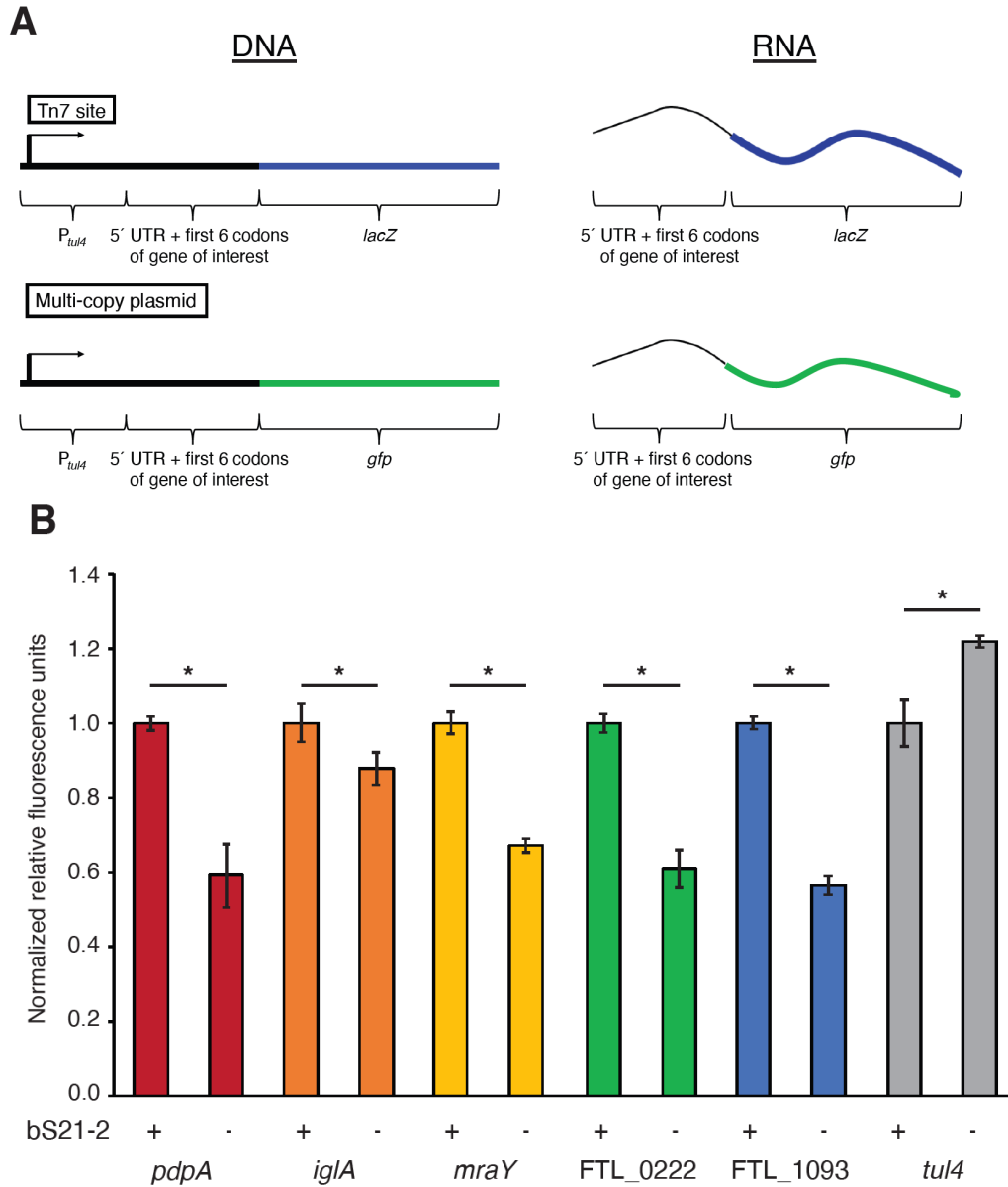


Figure 2. 5' UTRs are sufficient to lead to bS21-2-mediated changes in translation. (A) Diagrams of the translational reporter fusions used. Reporters used the *tul4* promoter to drive expression of the tested 5' UTR, including the first 6 codons of the gene, and are in frame with either *lacZ* at the Tn7 site of the genome or *gfp* on a multi-copy plasmid. **(B)** Relative fluorescence is reported for indicated translational fusion reporters in cells with (+; WT) or without (-; $\Delta rpsU2$) bS21-2 in biological triplicate. The *tul4* reporter serves as a control. 5' UTR sequences can be found in Table 1. Error bars represent 1 SD. * $p < 0.05$ by t-test. Experiments were repeated at least twice and data from a representative experiment are shown.

Figure 3. Genes with ideal Shine-Dalgarno (SD) sequences are not responsive to bS21-2. (A) bS21 interacts with the anti-Shine Dalgarno (ASD) sequence. In *E. coli*, the amino acid R17 of the sole bS21 protein (green) directly interacts with nt C1539 of the 16S, which is part of the ASD (blue). Measured distance is 2.7Å distance (PDB 6o7k visualized on PyMol v2.4; Kaledhonkar et al. 2019). **(B)** Introduction of an ideal SD in the *pdpA* leader leads to loss of bS21-2 responsiveness. Top: Relative β -galactosidase activity from modified or wild-type *pdpA* 5' UTRs in cells with (+; WT) or without (-; $\Delta rpsU2$) bS21-2, in biological triplicate. Bottom: Alignment of modifications to *pdpA* 5' UTR. Nucleotides altered from WT are capitalized; ideal SD sequences are in bold. **(C)** Introduction of an ideal SD in the *mraY* leader leads to loss of bS21-2 responsiveness. Top: Relative fluorescence is reported for indicated translational fusion reporters in cells with (+; WT) or without (-; $\Delta rpsU2$) bS21-2, in biological triplicate. Bottom: Alignment of indicated 5' UTRs; ideal SD sequences are in bold. Value in parenthesis indicates the number of identical nts omitted from 5' end of the UTRs. (B-C) Error bars represent 1 SD. * $p < 0.05$ by t-test. Ns = not significant. Experiments were repeated at least twice and data from a representative experiment are shown. **(D)** The absence of strong SD-ASD interactions is correlated with bS21-2 influencing translation. Fraction of genes that are positively-impacted (n=74), negatively-impacted (n=84), or unaffected (n=82) by bS21-2, categorized by strength of SD. "Strong" SD indicates 4 or more nts complementary to ASD; "weak" SD indicates 3 or fewer complementary nts.

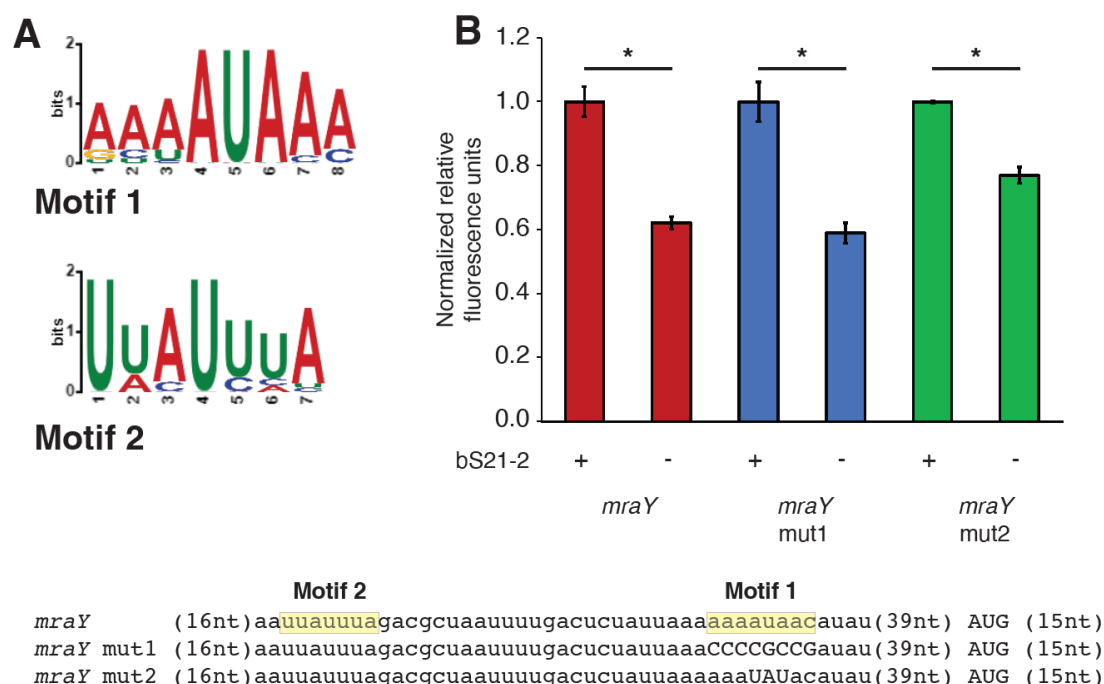


Figure 4. STREME-detected motifs are not necessary for bS21-2-responsive translation in the *mraY* 5' UTR. (A) Logos of two sequence motifs generated by STREME, found to be enriched in the 5' UTRs of the 20 most bS21-2-responsive genes compared to shuffled sequences. Motif 1 was detected in 19/20 input sequences; Motif 2 was detected in 18/20 input sequences. (B) Top: Relative fluorescence is reported for indicated translational fusion reporters in cells with (+; WT) or without (-; $\Delta rpsU2$) bS21-2, in biological triplicate. Error bars represent 1 SD. * $p < 0.05$ by t-test. Experiments were repeated twice and data from a representative experiment are shown. Bottom: Alignment of modifications to *mraY* 5' UTR. Nucleotides altered from WT are capitalized. Motifs are highlighted in yellow. Values in parenthesis indicates the number of identical nts omitted from the ends of the UTRs.

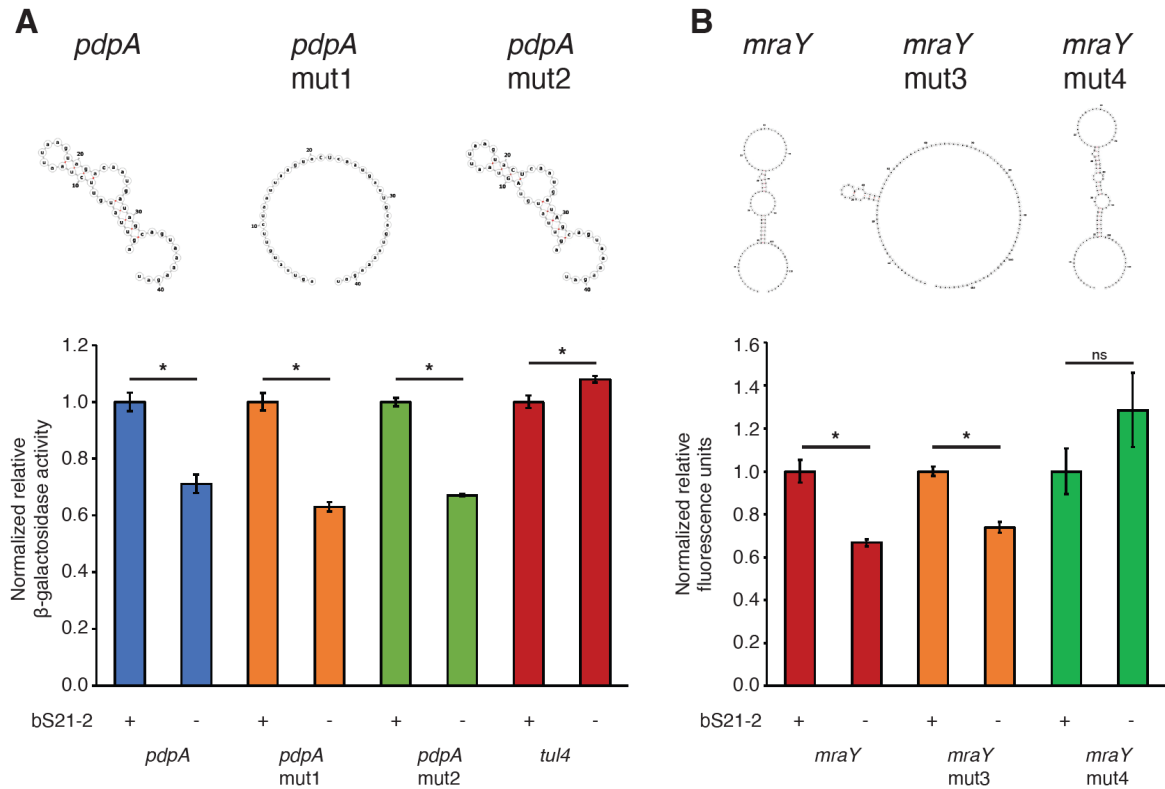


Figure 5. Predicted secondary structure plays no clear role in bS21-2-responsive translation. (A) Changing the *pdpA* secondary structure does not impact responsiveness to bS21-2. Top: Predicted secondary structures for wild-type and modified *pdpA* 5' UTRs, from MXFold2. Sequence modification can be found in Table 1. Bottom: Relative β -galactosidase activity from indicated 5' UTR fused to *lacZ*, in cells with (+; WT) or without (-; $\Delta rpsU2$) bS21-2, in biological triplicate. *tul4* is included as a control. **(B)** Changing the *mraY* secondary structure does not impact responsiveness to bS21-2. Top: Secondary structure predictions of wild-type and modified *mraY* 5' UTRs, from MXFold2. Sequence modification can be found in Table 1. Bottom: Relative fluorescence is reported for indicated translational fusion reporters in cells with (+; WT) or without (-; $\Delta rpsU2$) bS21-2, in biological triplicate. (A-B) Error bars represent 1 SD. * $p < 0.05$ by t-test. Experiments were repeated twice and data from a representative experiment are shown.

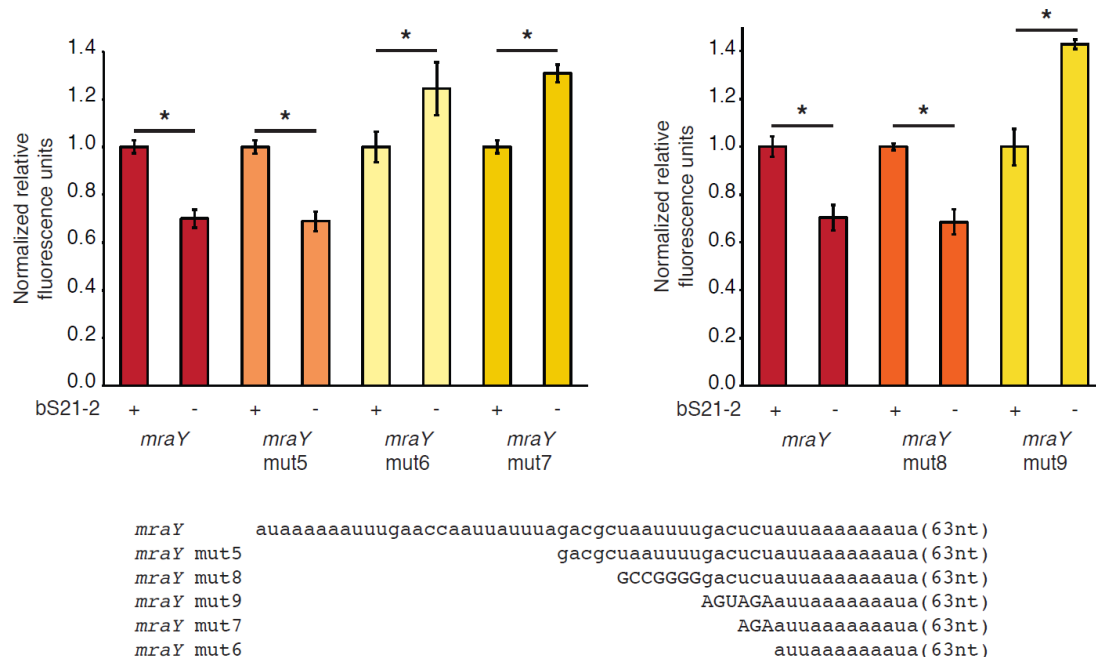


Figure 6. GACUCU is critical for bS21-2-mediated translation in the *mraY* 5' UTR. Top: Relative fluorescence is reported for indicated translational fusion reporters in cells with (+; WT) or without (-; $\Delta rpsU2$) bS21-2, in biological triplicate. Error bars represent 1 SD. * $p < 0.05$ by t-test. Experiments were repeated twice and data from a representative experiment are shown. Bottom: Alignment of modifications to *mraY* 5' UTR. Nucleotides altered from WT are capitalized. Values in parenthesis indicates the number of identical nts omitted from the 3' ends of the UTRs.

Supplemental Figures

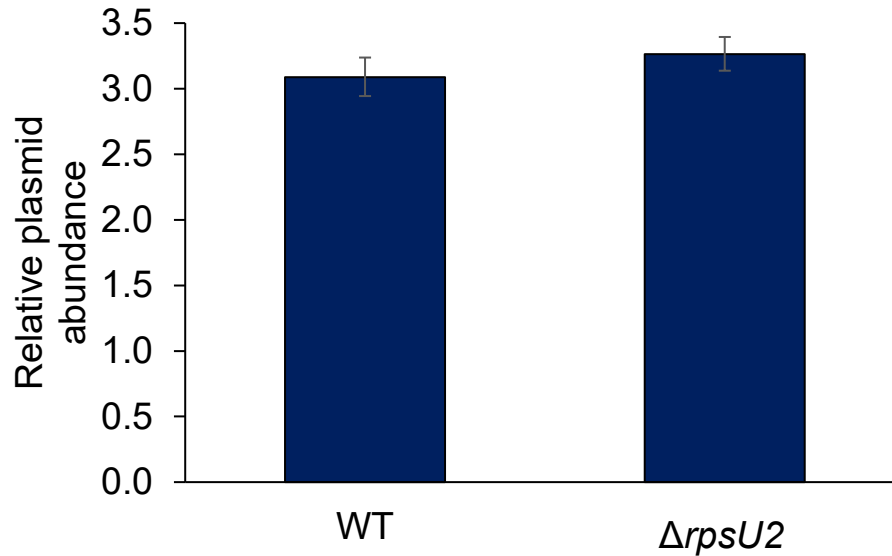


Figure S1. pF plasmid copy number is not affected by presence of bS21-2. Quantitative real-time PCR of total DNA from wild-type (WT) cells and cells lacking bS21-2 ($\Delta rpsU2$) was used to assess the relative abundance of the multi-copy pF plasmid used in GFP experiments. An opening reading frame on the plasmid, ORF3, was amplified and normalized to chromosomally-encoded *tul4*. Error bars represent 1 SD from the mean value (calculated using the mean threshold cycle). Experiments were repeated three times and data from a representative experiment are shown.

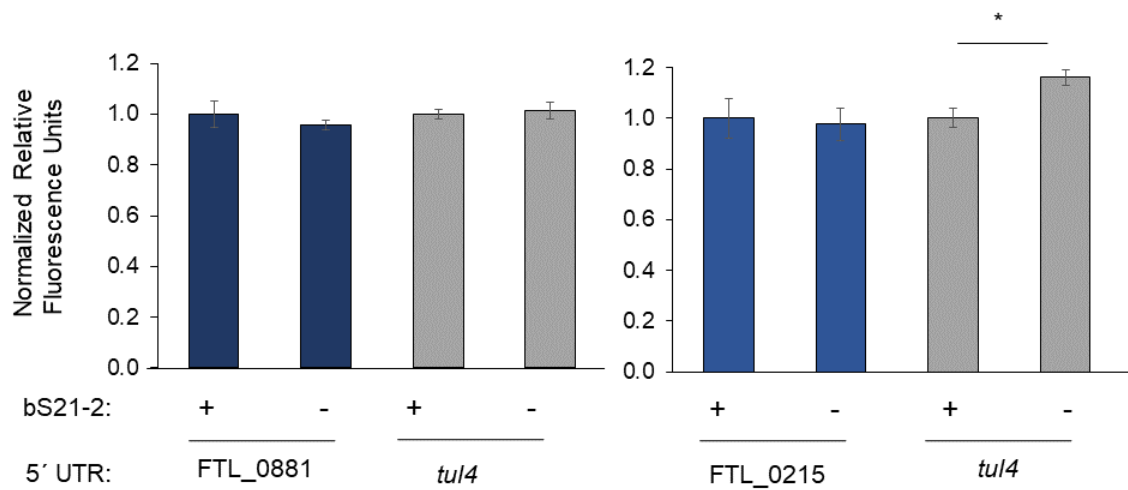


Figure S2. Some 5' UTRs do not lead to bS21-2-mediated changes in translation. Relative fluorescence is reported for indicated translational fusion reporters in cells with (+; WT) or without (-; $\Delta rpsU2$) bS21-2. FTL_0881 and FTL_0215 were found to be less abundant at the protein level in cells lacking bS21-2 in a proteomics screen (Trautmann & Ramsey, 2022). The *tul4* 5' UTR is included as a control. Error bars represent 1 SD. Experiments were repeated twice and data from representative experiments are shown. * p<0.05

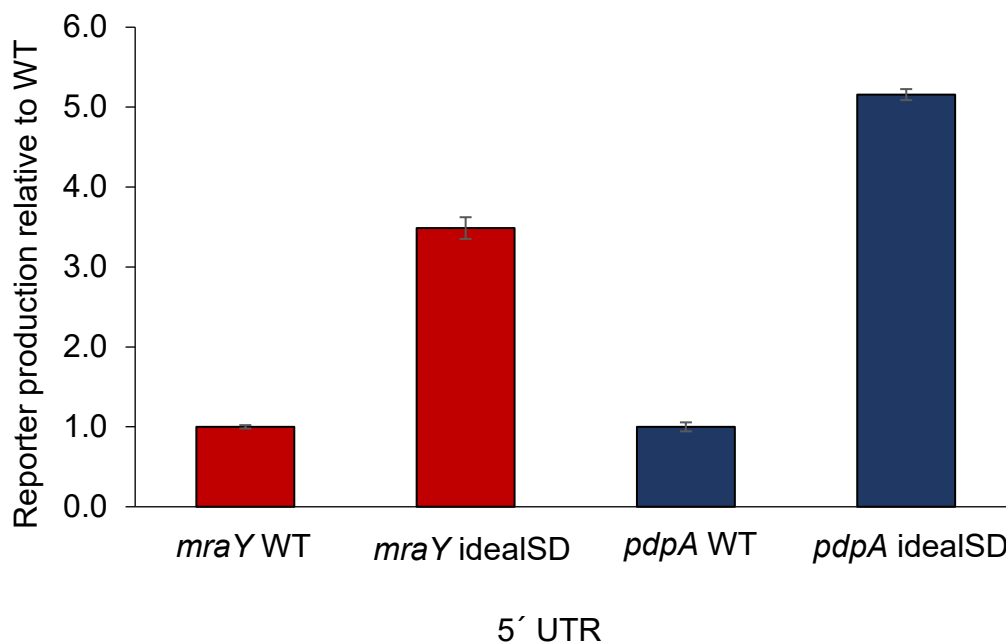







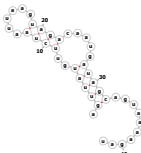
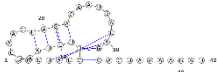


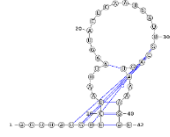



Figure S3. Addition of an ideal Shine-Dalgarno sequence increases reporter protein production relative to unmodified 5' UTRs. Relative β -galactosidase activity or fluorescence of *pdpA* or *mraY* 5' UTRs, respectively, in cells with bS21-2, compared to unmodified (WT) 5' UTR for each gene. Error bars represent 1 SD. Experiments were repeated twice and data from representative experiments are shown.

5' UTR	Sequence	MXFold2	Ufold	ViennaRNA
<i>mraY</i> WT	auaaaaaaaauuugaaccaauuuauu uagacgcuaauuuuugacucuauu aaaaaaaaaaacaauaucuauuuaua auacuccaaggucuuuaacauu uuaaaauauAUGcugauuuaucu uuuu			
<i>mraY</i> mut3	auaaaaaaaauuugaaccaauuuauu uagacgcuaauuuuugacucuauu aaaaaaaaaaacaauaucuauuuaua auacuccaCUACUauuuaaacau uuuaaaauau AUG cugauuuaucuuuuu		Server unavailable	
<i>mraY</i> mut4	auaaaaaaaauuugaaccaauuuauu uagacgcuaauuuuAGUGAGa uuaaaaaaaaaaacaauaucuauua uaaucuccaCUACUauuuaaac auuuuaaaauau AUG cugauuuaucuuuuu		Server unavailable	
<i>pdpA</i> WT	aguuauguucuaauuaaguagac aaugauagcaguaaaagau			
<i>pdpA</i> mut1	aguuauguucuaauuaaguaCU caaugauUgcaguaaaagau			

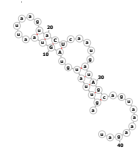
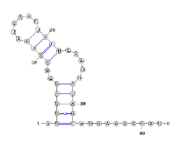

5' UTR	Sequence	MXFold2	Ufold	ViennaRNA
<i>pdpA</i> mut2	aguuauguAGuaauuaaguaCU caaugauAgcaguaaaaagau			

Figure S4. Comparison of secondary structure prediction software.

Predicted structures of wild-type or modified *mraY* and *pdpA* 5' UTRs from three secondary structure prediction programs: MxFold2 (Sato et al. 2021), Ufold (Fu et al. 2022), and ViennaRNA (Lorenz et al. 2011).